Robust synthetic aperture sonar for autonomous underwater vehicles

Roy Edgar Hansen

***Abstract*—The ocean environment can be challenging for synthetic aperture sonar (SAS) imaging. Running in rough topography cause severe deviations from ideal tracks, which again affects the imaging geometry. SAS is near field imaging, where the sound velocity must be estimated to maintain correct depth of focus. In ocean currents, crabbing may occur and non-straight synthetic apertures are formed. In shallow waters, multipath causes reduced quality in the SAS images, micronavigation and interferometry. In this paper, we discuss ways to increase robustness of SAS in challenging environments. We suggest that the SAS data collection should be environmentally adapted. This will improve the input data quality for SAS and thereby the overall robustness. For a given data collection, we suggest that the signal processing should be adapted to the actual collection. This will increase the ability to perform successful SAS and thereby the overall robustness. In all stages of the SAS processing there are choices on how to perform the different tasks. We discuss the different choices and their impact on quality and processing time. There is a tradeoff between robustness and efficiency in the environmentally adaptive data collection. There is a tradeoff between image quality and processing time in the data adaptive signal processing. Quality assessment is critical in robust adaptive SAS. Sonar coherence can be turned into an equivalent signal to noise measure. We show how this can be used as an effective quality estimate. We also show how to use sonar coherence in data interpretation.**

***Index Terms*—Synthetic aperture sonar, autonomous underwater vehicles**

I. Introduction

SYNTHETIC aperture sonar (SAS) technology is maturing rapidly. Today there are SAS systems commercially available from several companies. This allows for scientific development in new directions. Recently, new techniques have been developed in image enhancement [1], [2], advanced use of SAS in automatic target recognition (ATR) [3], more detailed analysis and interpretation of the geometry and scattering model [4] and new application areas [5], [6].

Another trend that follows naturally from increased operational use of SAS technology is the need for reliable SAS in any ocean environment. The Norwegian Defence Research Establishment (FFI) and Kongsberg Maritime have a long term collaboration to develop synthetic aperture sonar for the HUGIN autonomous underwater vehicle (AUV). The main sensor on the vehicle is the HISAS 1030 interferometric SAS [7], where special care has been taken for best possible performance in challenging environments [8], [9]. The first HUGIN 1000-MR AUV was delivered to the Royal Norwegian Navy (RNoN) in mid-2008. Fig. 1 shows the HUGIN 1000-MR during recovery onboard the RNoN mine hunter Hinnøy. FFI has a close collaboration with the RNoN and Kongsberg Maritime in developing robust SAS for military AUV operations. RNoN serves as a pilot user always being early in exploring and pushing the true limitations of SAS and AUV technology.

Norwegian Defence Research Establishment, P. O. Box 25, NO-2027 Kjeller, Norway. E-mail: Roy-Edgar.Hansen@ffi.no.

Fig. 1. HUGIN 1000-MR AUV with HISAS 1030 during recovery on the Royal Norwegian Navy mine hunter Hinnøy.

Successful SAS requires sufficient knowledge of the ocean environment, the imaging geometry and the vehicle navigation. In this paper, we list the requirements and discuss the impact of vehicle stability, terrain, ocean currents, sound velocity errors and the sea surface in shallow waters.

We show several ways to improve the quality of the data collected for SAS and bathymetry processing for different types of ocean environment.

When data has been properly collected, the final step in successful SAS is intelligent use of the data in the signal processing. We discuss in detail some of the possible choices in data adaptive signal processing. A crucial component of robust autonomous SAS is the possibility to assess quality reliably. We describe how to use coherence in quality assessment.

II. Data collection requirements

A. Requirements

Successful SAS is dependent of a number of requirements to be met:

1) The synthetic aperture has to be well sampled. This restricts the distance travelled between each ping [10] and

thereby the area coverage rate [11]. For multi-element receiver array systems, the pings can be collected such that there is a certain redundancy or *overlap* in the synthetic aperture [12]. The overlap can be used in micronavigation [13].

2) The direction of each element in sonar has to be such that each pixel in the imaging scene has to be insonified by each element in the synthetic aperture. This restricts the attitude variations of the sonar array over the synthetic aperture, and the sampling of the synthetic aperture.

3) The position of each element along the synthetic aperture has to be positioned within a fraction of a wavelength at the highest frequency. This requirement is generally not met even with advanced inertial navigation on AUVs, except for very low acoustic frequencies.

4) For non-straight synthetic apertures the full imaging geometry must be known within bounds [14], [15]. This implies that seafloor depth in the imaging swath must be estimated during the SAS processing or known as a input from a digital terrain model. For perfect straight line synthetic apertures, the imaging geometry becomes cylinder symmetric and invariant of the bathymetry.

5) SAS is near-field imaging. This implies that the sound velocity profile (SVP) from sensor position to seafloor imaging pixel, has to be known within a certain accuracy [16], [17]. An incorrect SVP will cause defocusing in the SAS image even with perfect navigation.

6) When operating in waters with ocean currents or on badly trimmed vehicles, crabbing (or differences between receiver array direction and track direction) can occur. This will generate non-straight apertures and non-zero baselines for overlapping phase centers (in micronavigation [13]).

7) In shallow waters, sound waves may be reflected in the sea surface [18] and thereby affect the SAS processing in several ways: the spatial coherence becomes lower [19] and thereby the ability to map the scene; the temporal coherence becomes lower and limits the micronavigation performance; the multipath (or clutter) becomes higher in the SAS image, and lowers the image quality.

B. Environmentally adaptive data collection

To ensure the highest possible quality in the output images and bathymetries in the SAS processing, the data should be collected intelligently – that is – adapted to the environment and the mission goal. Fig. 2 shows a basic flowchart for intelligent environmentally adaptive data collection. The data quality can be improved during collection in several ways:

1) In shallow waters, the vehicle should choose a depth and a sonar setting that ensures maximum range [9], [19]. The overlap should also be increased to mitigate the effect of multipath. The true range of the sensor should be estimated [19], and the track spacing in the survey pattern should then be adjusted to the corrected sensor range.

2) In range limited environments, such as shallow waters with multipath, the vehicle can increase speed until the data collection range swath matches the achievable range such that the area coverage is increased [11].

3) In waters with ocean currents, there are several choices [20]: the vehicle can run upstream and downstream to reduce

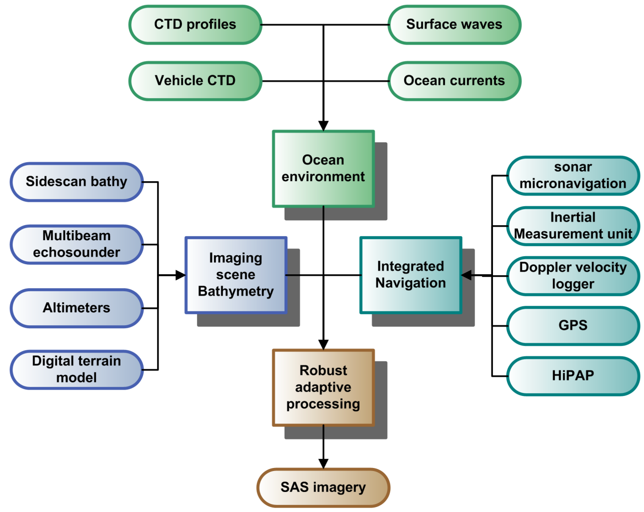

Fig. 2. Robust SAS data collection scheme.

crabbing; the vehicle can run faster to reduce crabbing. If crabbing cannot be avoided, the distance between pings should be reduced such that the negative effects of crabbing are acceptable. Reduced distance between pings increase the overlap, but reduces the area coverage rate.

4) In waters with varying sound velocity (typically in the littoral during the summer months), special care should be made to collect enough information about the SVP (sufficient sampling in space and time). This can be done by using the onboard CTD on the vehicle, potentially in combination with CTD profiles from other platforms (the vessel) [17]. Note that, ideally the entire profile is required, while for typical AUV-operations only the SVP from surface to vehicle depth is recorded. This means that the vehicle should take a full profile often enough to ensure sufficient sampling.

5) In rough terrain where straight line synthetic apertures are impossible, the track deviations from a straight line should be as smooth as possible. This eases the requirement on map accuracy [9], [15]. Then sufficient map resolution and accuracy should be ensured. For a given track, it is straight-forward to calculate the required map accuracy [15]. The map accuracy can be increased by operating the mapping sensors differently, e.g. reducing range for the interferometric sidescan or running densely spaced mission lines to obtain full coverage with the multibeam echosounder.

6) When limited by navigation accuracy, micronavigation performance should be adjusted to ensure sufficient total navigation accuracy. The overlap factor (the number of overlapping phase centers) should be adapted to the needed accuracy [13]. This affects directly the achievable range.

C. Tradeoffs in data collection

There is a clear tradeoff between sensor effectiveness and resolution on one hand, and robustness on the other hand. More robust data collection implies more redundancy or overlap, and thereby lower effectiveness given by area coverage rate.

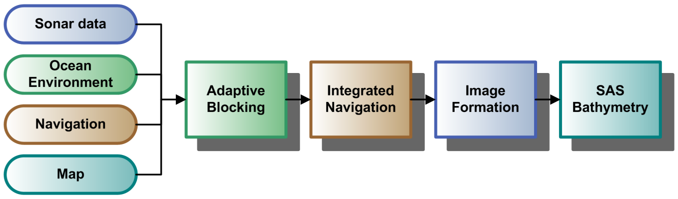

Fig. 3. SAS processing flow.

III. Robust SAS processing

SAS signal processing can be divided into four parts, as shown in Fig. 3:

1) SAS forms a 2D image of a selection of pings, or a block of data. The adaptive blocking divides the pings into suitable blocks where each block forms one image. See section III-A for details.

2) If the navigation accuracy is not sufficiently high, micronavigation [13] can be integrated with inertial navigation [21]. Alternatively, this can be done after image formation using autofocus techniques [14], [22].

3) The SAS image is then constructed by coherent combination of all pings in the block. The choice of beamformer for this task, is dependent of the sensor parameters and the vehicle track.

4) For interferometric systems such as the HISAS 1030, there are two or more receiver arrays with a cross-track baseline. Coherent comparison of the SAS images from these sensors, can then be used to estimate a high resolution bathymetric map. This requires that the images are phase coherent and contain single scattering echoes from the seafloor and that coregistering is feasible.

In all these stages there are a number of choices in how the processing can be made. Which choice is optimal is dependent of the actual data collection. Other requirements such as real-time factor (or processing speed) also affects the choice of method. Requirements for successful synthetic aperture processing is discussed in detail in [22], [23].

A. Data adaptive signal processing

The adaptive blocking the SAS signal processing flow as shown in Fig. 3 is a crucial part of the processing chain. There are several choices to be made on how to do the SAS processing. The level of adaptivity – or how many parameters should be changed adaptively – is also a choice. With reference to Fig. 4, we divide the decision making that can be made adaptive into 6 parts:

Track linearity checks for sufficiently straight lines within a mission line. The mission line is divided into blocks where separate SAS images are formed from each block.

Vehicle stability checks the vehicle stability preferrably in form of small scale attitude rates and deviations from straight lines. The output from this is a suggested motion compensation technique (for wavenumber based imaging techniques) and imaging technique. A perfect straight line with fairly narrow beams would allow for using the chirp-scaling algorithm in beamforming, while a heavily non-straight synthetic aperture in combination with a wideband widebeam sensor might require the backprojection beamformer. If the vehicle is highly unstable – having high frequency vibrations and attitude changes, this might imply that the backprojection has to be fully bistatic using the actual transmitter position during transmit and the actual receiver array position during reception (i.e. range dependent navigation within ping).

Crab analysis monitors the vehicle crabbing and chooses suitable micronavigation strategy and beamformer [20], [24]. Large crabbing angles implies large baselines in the overlapped phase centers, which again affects the performance of micronavigation and also choice of navigation strategy (see *navigation accuracy* for further details).

Terrain variation and accuracy calculates the specific need for accuracy in maps and checks the availability for the required accuracy. The required accuracy is function of the synthetic aperture track [15]. If the map is not sufficiently accurace, iterative techniques can be used to improve the map accuracy in interferometry. A Digital Terrain Model (DTM) from all relevant sensors [25] from all relevant lines, might be used to improve map accuracy. Under extreme requirements such as for circular apertures [4], [26], belief propagation [27] or similiar techniques might be the only choice.

Sound velocity variation and accuracy observes sound velocity profile (SVP) variations in the data collection. If the SVP is found to be too inaccurate, autofocusing can be used to correct imagery and estimate the error in the SVP in some cases [17]. There are cases where this might be difficult. If the synthetic aperture (from the blocking) actually goes through too large SVP variations (due to vertical displacement or other factors), wavenumber type imaging techniques cannot be used without modification since these techniques use constant sound velocity assumption in the full scene. Then a choice can be to use this information in re-blocking the data

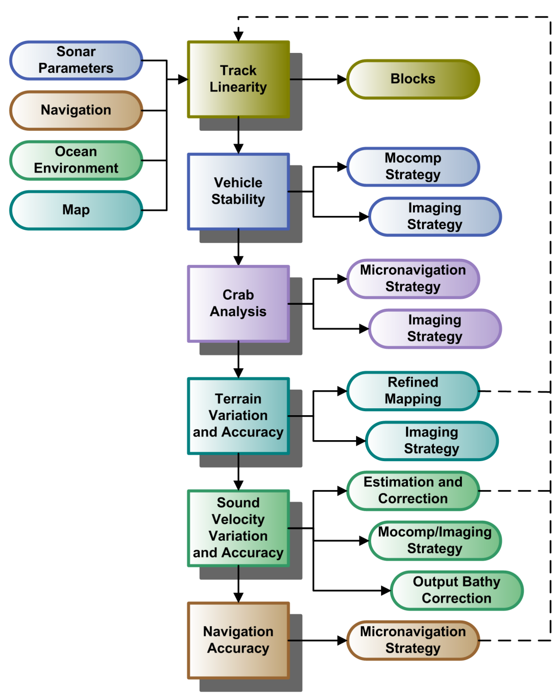

Fig. 4. Adaptive decision making in the SAS processing.

(as indicated in the figure).

Navigation accuracy calculates the required navigation accuracy and monitors the available predicted navigation accuracy (from the real-time or post processed navigation output [9], [28]). If the accuracy requirement is not met, a micronavigation technique can be chosen. We have developed three different techniques with different performance and processing speed: Micronavigation on sway and heave only after motion compensation (2. order DPCA as we refer to it) [29] is very fast and accurate but not very robust. Micronavigation using DPCA [13], [21] is more robust but slower. Coherent correlation of ping-to-ping images in ground-range earth fixed coordinates (3. order DPCA as we refer to it) has the potential to be even more accurate and robust [26].

B. Tradeoffs in signal processing

In SAS signal processing there is a trade-off between image quality and resolution on one hand, and computational load or real-time factor on the other hand.

Synthetic aperture image formation is all about attention to detail. The required output quality affects the choice of algorithm: higher resolution requires more accurate methods; higher image quality (e.g. signal to noise ratio) requires more accurate methods. More advanced products such as interferometry requires much higher phase accuracy in the processing. All these factors affect the processing speed and software complexity.

There is also a tradeoff between quality and real-time factor given by other factors than SAS itself. After a survey of an area, the entire data set can be used in obtaining higher navigation accuracy by post processing of the navigation [28], [30]. The entire data collection from all mapping sensors can also be used to produce a more complete and better map for use in SAS. This implies that post mission SAS processing has the potential to be better than any in-mission processing.

IV. Quality Assessment

An important part of robust adaptive SAS is the ability to assess performance or quality. One candidate for assessing quality is the coherence which can be calculated as follows. Assume two receivers spatially and/or temporally displaced that record emitted signals (e.g. a scattered field from a rough surface) s_1 and s_2. The *mutual coherence function* is defined as [31, pp 499–503], [32, p 170]

$$\Gamma_{12}(\tau) = \langle s_1(t) s_2^*(t+\tau) \rangle \tag{1}$$

The *complex degree of coherence* is the normalized mutual coherence function

$$\gamma_{12}(\tau) = \frac{\Gamma_{12}(\tau)}{[\Gamma_{11}(0)\Gamma_{22}(0)]^{1/2}} \tag{2}$$

with the property that

$$0 \leq |\gamma_{12}(\tau)| \leq 1. \tag{3}$$

The coherence as used in the radar literature [33], [34] is usually referred to as the peak value in this function

$$\gamma = \arg\max_{\tau} \gamma_{12}(\tau). \tag{4}$$

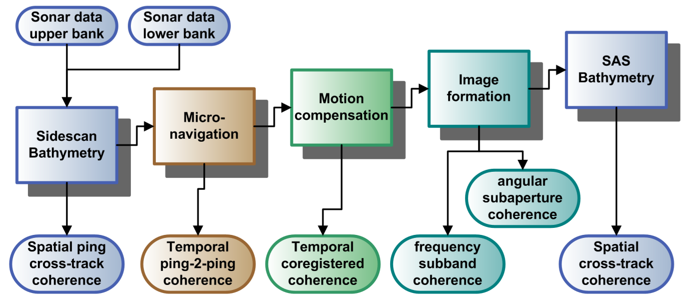

Fig. 5. Quality assessment using sonar coherence in different places in the processing chain.

The coherence can be converted to an equivalent signal to noise ratio under certain assumptions [33], [35]

$$\text{SNR} = \frac{|\gamma|}{1-|\gamma|}. \tag{5}$$

Coherence can be calculated different places in the SAS processing chain, as illustrated in Fig 5. Ping based (or real aperture) interferometric coherence can be calculated using beamformed timeseries from the upper and lower array. This can be used directly to estimate the depth accuracy in the sidescan interferometry map [25]. Ping to ping temporal coherence can be calculated if there are overlapped phase centers (for use in micronavigation). A similar temporal coherence can be calculated after motion compensation [29].

Both the temporal ping to ping coherence and the spatial ping based coherence are sensitive to multipath and can be used to map the actual performance or range in shallow waters [19]. Fig 6 shows the sidescan image and the sidescan bathymetry coherence from mission line collected in shallow waters. We see that there are areas of high backscatter but low coherence. This indicates multipath – which is not easy to spot from the sidescan image alone. Note also that the range for which the coherence is high, varies a lot during the mission line. This indicates that true sensor range has to be estimated based on the data itself.

Another potential application of coherence is to use the equivalent SNR calculated from coherence in the assessment of detection and classification performance [36].

A new and very promising use of spatio-temporal coherence is mapping of the coherence between mission lines [37]. This has the potential to dramatically improve navigation and to be the enabling technology to manage repeat-pass interferometry and coherent change detection.

When forming a synthetic aperture, the aperture coherence or generalized coherence factor can be calculated [38]. This is defined as the coherent energy divided by the incoherent energy over the array. A similar technique can be used to calculate the frequency coherence. These two coherences cannot be used to assess quality, but rather be used in characterisation. The reason for this is that a fully developed speckle scene will have very low aperture and frequency coherence since speckle does not fulfill the holographic property [14].

For interferometric SAS, the final quality assessment can be made on the SAS interferometry spatial coherence. This is the ultimate SAS quality since it is gridded directly in

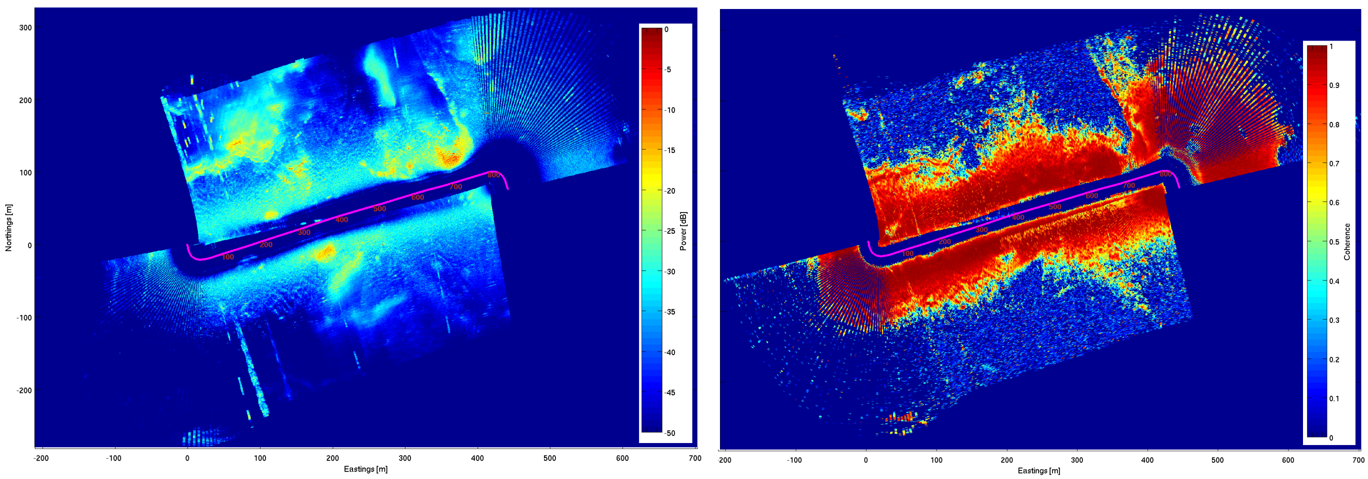

Fig. 6. Example sidescan sonar image (left) with sonar coherence (right) of a mission line collected in shallow waters. The vehicle depth is 5 m and the seafloor depth is around 18 m except in the norht-east corner, where the depth increases to 32 m. The image is shown in earth fixed coordinates.

the coordinate system of the SAS image with a very high horizontal resolution. Fig 7 shows an example SAS image of an unknown rectangular object on the seafloor. The object is quite large measuring $15 \times 5 \times 2$ m. The left panel shows the SAS image, the middle panel shows the SAS bathymetry and the right panel shows the magnitude coherence. The object is observed with the port side sonar on HUGIN AUV at approximately 52 m range, when running at 10.8 m altitude. We see that the coherence is low in the shadow region, as expected. The coherence is, however, low in the near range of the object too (at $y = [-43, -47]$ m). We also note that the measured depth seems incorrect and the backscatter signal is high in this region. This combination: front end of an elevated target with incorrect bathymetry, low coherence, and high backscatter, indicates an area of multiple reflections [4]. From this example we see that interferometric coherence can be used to obtain a higher understanding of the true information content in a SAS image.

V. Summary

Successful SAS operations requires sufficient knowledge of the ocean environment, the imaging geometry and the vehicle navigation. SAS is more challenging when running on non-straight lines and/or on instable vehicles. SAS is more challenging when running in an ocean environment with large variations in sound velocity and large ocean currents.

There are several ways to improve the data collection such that better performance is achieved. This includes adapting the vehicle behaviour and the sonar settings to the environment. There is a tradeoff between robustness and efficiency in the data collection of SAS data. Higher robustness implies lower area coverage rate.

There are many different choices in the SAS processing. The best choice is dependent on the actual data collected. There is a tradeoff between quality and processing time in the signal processing. Better quality requires more processing time.

Acknowledgment

The author wish to thank the Royal Norwegian Navy Mine Warfare Service for providing enourmous amounts of SAS data from challenging areas. The author also thanks Kongsberg Maritime for a long and fruitful collaboration. The author would finally like to thank the rest of the SAS team at FFI, Hayden J Callow, Torstein O Sæbø and Stig A V Synnes for fruitful discussions during this work.

References

[1] J. Groen, R. E. Hansen, H. J. Callow, J. C. Sabel, and T. O. Sæbø. Shadow enhancement in synthetic aperture sonar using fixed focusing. *IEEE J. Oceanic Eng.*, 34(3):269–284, 2009.

[2] R. E. Hansen, H. J. Callow, T. O. Sæbø, P. E. Hagen, and B. Langli. High fidelity synthetic aperture sonar products for target analysis. In *Proceedings of Oceans '08 Quebec*, Quebec, Canada, September 2008.

[3] E. Coiras and J. Groen. 3D target shape from SAS images based on a deformable mesh. In *Proceedings of Underwater Acoustic Measurements 2009*, Nafplion, Greece, June 2009.

[4] H. J. Callow, S. A. V. Synnes, T. O. Sæbø, and R. E. Hansen. Autofocus for circular synthetic aperture imaging. In *Proceedings of Synthetic Aperture Sonar and Radar 2010*, Lerici, Italy, September 2010.

[5] R. E. Hansen, P. E. Hagen, and H. S. Telle. Synthetic aperture sonar: a tool in underwater archaeology. In *Proceedings of Underwater Acoustic Measurements 2009*, Nafplion, Greece, June 2009.

[6] R. E. Hansen, T. O. Sæbø, H. J. Callow, and P. E. Hagen. Interferometric synthetic aperture sonar in pipeline inspection. In *Proceedings of Oceans 2010 MTS/IEEE*, Sydney, Australia, May 2010.

[7] P. E. Hagen, T. G. Fossum, and R. E. Hansen. HISAS 1030: The next generation mine hunting sonar for AUVs. In *UDT Pacific 2008 Conference Proceedings*, Sydney, Australia, November 2008.

[8] P. E. Hagen and R. E. Hansen. Synthetic aperture sonar challenges ... and how to meet them. *Hydro International*, pages 26–31, may 2008.

[9] P. E. Hagen and R. E. Hansen. Robust synthetic aperture sonar operation for AUVs. In *Proceedings of Oceans '09 MTS/IEEE Biloxi*, Biloxi, MS, USA, October 2009.

[10] M. P. Bruce. A processing requirement and resolution capability comparison of side-scan and synthetic-aperture sonars. *IEEE J. Oceanic Eng.*, 17(1):106–117, 1992.

[11] P. E. Hagen and R. E. Hansen. Area coverage rate for synthetic aperture sonars. In *Proceedings of Oceans '07 Europe*, Aberdeen, Scotland, June 2007.

[12] M. A. Pinto. High resolution seafloor imaging with synthetic aperture sonar. *IEEE Oceanic Eng. Newsletter*, pages 15–20, Summer 2002.

[13] A. Bellettini and M. A. Pinto. Theoretical accuracy of synthetic aperture sonar micronavigation using a displaced phase-center antenna. *IEEE J. Oceanic Eng.*, 27(4):780–789, 2002.

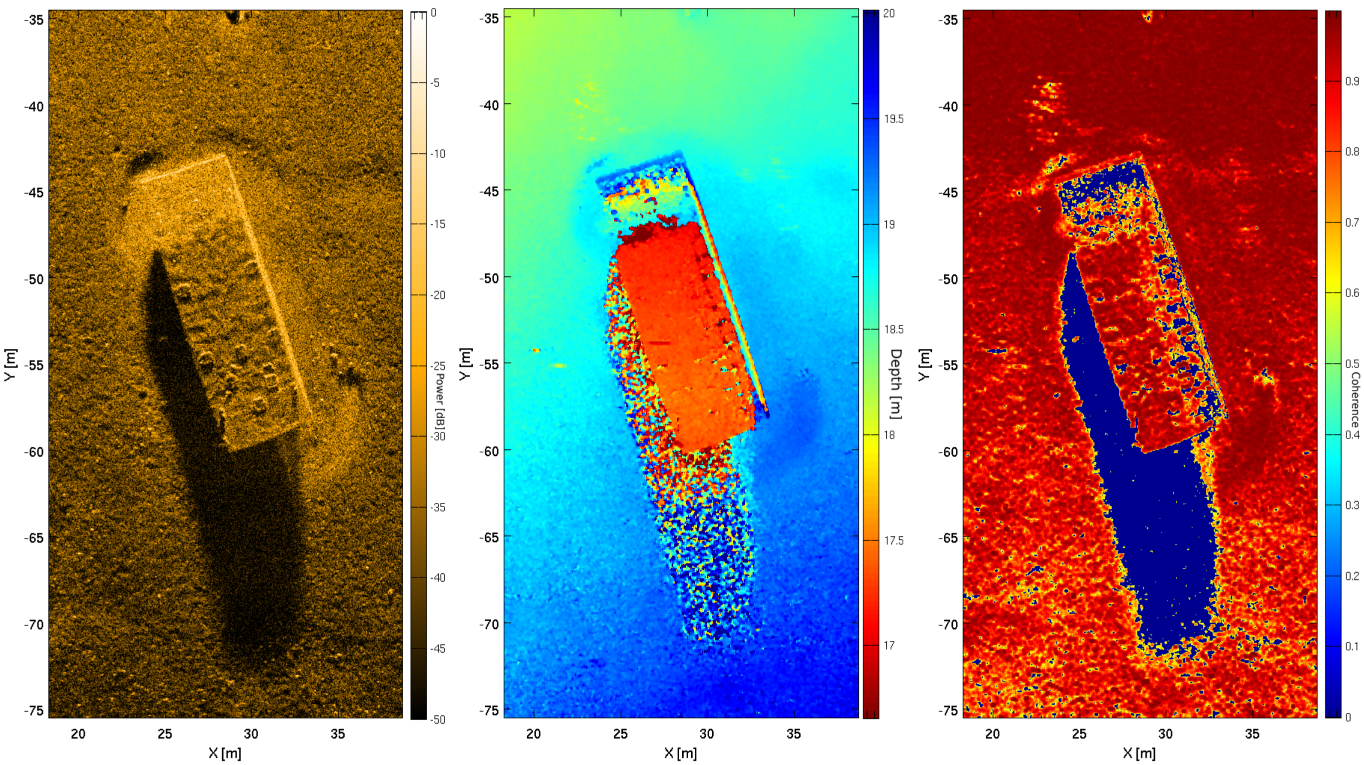

Fig. 7. SAS image of a 15 x 5 m rectangular object on the seafloor. The range is 52 m and the vehicle altitude is 10.8 m. The vehicle moves from left to right (along positive x-axis). The left panel shows the SAS image. The theoretical resolution is 3.7×3.2 cm. The middle panel shows the SAS bathymetry with color coded depth. The object is approximately elevated 1.8 m above the seafloor. This fits well the data collection geometry and the length of the shadow. The right panel shows the magnitude coherence. The coherence is low in the shadow region and in the layover and multi-bounce region.

[14] J. C. V. Jakowatz, D. E. Wahl, P. H. Eichel, D. C. Ghiglia, and P. A. Thompson. *Spotlight-Mode Synthetic Aperture Radar: A Signal Processing Approach*. Kluwer Academic Publishers, 1996.

[15] R. E. Hansen, H. J. Callow, T. O. Sæbø, S. A. Synnes, P. E. Hagen, T. G. Fossum, and B. Langli. Synthetic aperture sonar in challenging environments: Results from the HISAS 1030. In *Proceedings of Underwater Acoustic Measurements 2009*, Nafplion, Greece, June 2009.

[16] K. D. Rolt and H. Schmidt. Effects of refraction on synthetic aperture sonar imaging. *J. Acoust. Soc. Am.*, 95(6):3424–3429, 1994.

[17] R. E. Hansen, H. J. Callow, and T. O. Sæbø. The effect of sound velocity variations on synthetic aperture sonar. In *Proceedings of Underwater Acoustic Measurements 2007*, Crete, Greece, June 2007.

[18] X. Lurton. *An Introduction to Underwater Acoustics: Principles and Applications*. Springer Praxis Publishing, 2002.

[19] S. A. Synnes, R. E. Hansen, and T. O. Sæbø. Assessment of shallow water performance using interferometric sonar coherence. In *Proceedings of Underwater Acoustic Measurements 2009*, Nafplion, Greece, June 2009.

[20] P. E. Hagen, T. G. Fossum, H. J. Callow, R. E. Hansen, and Choi J. L. Synthetic aperture sonar operation in challenging environments: Experiences from HUGIN 1000 operations around the world. In *UDT Europe 2010 Conference Proceedings*, Hamburg, Germany, June 2010.

[21] R. E. Hansen, T. O. Sæbø, K. Gade, and S. Chapman. Signal processing for AUV based interferometric synthetic aperture sonar. In *Proceedings of Oceans 2003 MTS/IEEE*, volume 5, pages 2438–2444, San Diego, CA, USA, September 2003.

[22] W. G. Carrara, R. S. Goodman, and R. M Majewski. *Spotlight Synthetic Aperture Radar: Signal Processing Algorithms*. Artech House, 1995.

[23] D. A. Cook and D. C. Brown. Analysis of phase error effects on stripmap SAS. *IEEE J. Oceanic Eng.*, 34 (3):250–262, 2009.

[24] H. J. Callow. Comparison of sas processing strategies for crabbing collection geometries. In *Proceedings of Oceans 2010 MTS/IEEE*, Seattle, US, September 2010.

[25] T. O. Sæbø and B. Langli. Comparison of EM 3000 multibeam echo sounder and HISAS 1030 interferometric synthetic aperture sonar for seafloor mapping. In *Proceedings of European Conference on Underwater Acoustic (ECUA) 2010*, Istanbul, Turkey, July 2010.

[26] H. J. Callow, R. E. Hansen, S. A. Synnes, and T. O. Sæbø. Circular SAS without a beacon. In *Proceedings of Underwater Acoustic Measurements 2009*, Nafplion, Greece, June 2009.

[27] P.J. Barclay, C.J. Forne, M.P. Hayes, and P.T.; Gough. Reconstructing seafloor bathymetry with a multichannel broadband insas using belief propagation. In *Proceedings of Oceans 2003 MTS/IEEE*, volume 4, pages 2149–2154, San Diego, CA, USA, September 2003.

[28] B. Jalving, K. Gade, O. K. Hagen, and K. Vestgård. A toolbox of aiding techniques for the HUGIN AUV integrated inertial navigation system. In *Proceedings of Oceans 2003 MTS/IEEE*, San Diego, CA, USA, September 2003.

[29] H. J. Callow, T. O. Sæbø, and R. E. Hansen. Towards robust quality assessment of SAS imagery using the DPCA algorithm. In *Proceedings of Oceans '05 Europe*, Brest, France, June 2005.

[30] K. Gade. NAVLAB, a generic simulation and post-processing tool for navigation. *European Journal of Navigation*, 2(4):51–59, 2004.

[31] M. Born and E. Wolf. *Principles of Optics*. Pergamon press, 1999.

[32] J. W. Goodman. *Speckle phenomena in optics: theory and applications*. Roberts and Company, 2007.

[33] R. F Hanssen. *Radar Interferometry: Data Interpretation and Error Analysis*. Kluwer Academic Publishers, 2001.

[34] R. Touzi, A. Lopes, J. Bruniquel, and P. W. Vachon. Coherence estimation for sar imagery. *ieeegrs*, 37(1):135–149, January 1999.

[35] H. A. Zebker and J. Villasenor. Decorrelation in interferometric radar echoes. *IEEE Trans. Geosci. Remote Sensing.*, 30(5):950–959, 1992.

[36] Ø. Midtgaard, T. O. Sæbø, and R. E. Hansen. Estimation of detection/classification performance using interferometric sonar coherence. In *Proceedings of Underwater Acoustic Measurements 2009*, Nafplion, Greece, June 2009.

[37] S. A. V. Synnes, H. J. Callow, T. O. Sæbø, and R. E. Hansen. Multipass coherent processing on synthetic aperture sonar data. In *Proceedings of European Conference on Underwater Acoustic (ECUA) 2010*, Istanbul, Turkey, July 2010.

[38] P. C. Li and M. L. Li. Adaptive imaging using the generalized coherence factor. *IEEE Trans. Ultrason. Ferroelect. Freq. Contr.*, 50(2):128–141, 2003.